

RUSLE-BASED GEOSPATIAL ASSESSMENT OF SOIL EROSION FOR CONSERVATION PLANNING AT THE NATIONAL ROOT CROPS RESEARCH INSTITUTE (NRCRI), UMUDIKE, NIGERIA

Uzor-Totty A. E., Chukwuemeka O. S., Edoh C. Eluwa J. C., & Adiele-Ezekiel C.

Agrometeorological Unit, National Root Crops Research Institute.



Corresponding Author's Email: auzortotty@gmail.com; amara.uzo-totty@nrcri.gov.ng

Abstract

<https://doi.org/10.65760/sjgs.v4.i1.1>

Soil erosion poses a significant threat to agricultural sustainability in the humid tropical zone. This study employs the Revised Universal Soil Loss Equation (RUSLE) integrated with Geographic Information Systems (GIS) and remote sensing to quantitatively assess soil erosion rates and identify critical risk areas within the National Root Crops Research Institute (NRCRI), Umudike. Key factors, rainfall erosivity (R), soil erodibility (K), topography (LS), cover-management (C), and support practices (P), were derived from field data, laboratory analysis, satellite imagery (Sentinel-2), and a 30m SRTM DEM, respectively. Results revealed substantial spatial variation in annual soil loss, with rates increasing significantly on steep slopes under intensive root-crop cultivation and minimal cover. Sensitivity analysis identified the topographic (LS) and cover-management (C) factors as the dominant drivers, collectively explaining 70-80% of the variation in erosion. The study maps out high-priority erosion hotspots and provides a foundational, spatially explicit evidence base for targeted conservation planning. Recommendations from the study include prioritizing terracing and contour farming on steep slopes, enhancing vegetative cover through improved crop management practices, and establishing a monitoring framework using the developed RUSLE-GIS model.

Keywords: RUSLE, Geospatial Analysis, GIS/Remote Sensing, Conservation Planning, Soil Erosion and Nigeria.

1.1 Introduction

Soil erosion, recognized as the primary form of global land degradation, presents a profound threat to agricultural sustainability, water resources, and food security worldwide (ELD Initiative & UNEP, 2015). It is driven by the dynamic forces of water and wind, and significantly accelerated by anthropogenic activities such as unsustainable farming, deforestation, and land development (Pimentel, 2006; FAO & ITPS, 2015). The consequences are staggering; recent estimates indicate that approximately 1.9 billion hectares or 65% of the planet's soils are degraded, with erosion alone accounting for 85% of this damage (WEF, 2020). This results in the annual loss of over 36 billion tonnes of fertile soil, with an associated economic cost reaching \$400 billion. This crisis threatens the livelihoods of the 1.5 billion people who depend directly on degraded agricultural land, creating a pressing need for accurate assessment and effective intervention.

Globally, soil erosion manifests differently across regions, reflecting variations in climate, topography, land use, and management practices. In Asia, intensive agricultural systems on steep slopes, particularly in the Himalayan foothills and the Loess Plateau of China, experience severe erosion rates exceeding $100 \text{ t ha}^{-1} \text{ yr}^{-1}$ in some locations (Pimentel et al., 1995). South America faces

significant challenges from deforestation of the Amazon basin and expansion of soybean and cattle production, which accelerate erosion on previously forested lands (Panagos et al., 2015). Europe experiences widespread soil degradation, with the Mediterranean region being particularly vulnerable due to prolonged drought periods followed by intense rainfall, coupled with centuries of agricultural modification (Renard et al., 1997). North America has made substantial progress in erosion control following the Dust Bowl era; however, regions such as the Midwest Corn Belt continue to experience soil loss rates exceeding tolerance thresholds (Prasannakumar et al., 2012). Australia's ancient, weathered soils remain highly susceptible to erosion, particularly during drought cycles that remove protective vegetation cover (Mitasova et al., 2013).

Across the African continent, the erosion crisis is particularly acute due to the convergence of high climatic variability, expanding agricultural frontiers, and limited institutional capacity for conservation planning. Sub-Saharan Africa experiences some of the world's highest erosion rates, with estimated average soil loss of 30-50 t ha⁻¹ yr⁻¹ in intensively cultivated zones (Lal, 2001). East Africa, including Ethiopia and Kenya, suffers from severe gully erosion that permanently removes land from agricultural production and destabilizes infrastructure (Anejionu et al., 2013). Southern Africa faces challenges from both water and wind erosion, with climate change projections indicating increased rainfall intensity that will exacerbate these processes. West Africa, particularly the Guinea savanna and forest transition zones, experiences high erosion rates driven by the replacement of perennial vegetation with annual row crops, combined with the removal of crop residues for fuel and fodder (FAO & ITPS, 2015). Despite the severity of these challenges, many African nations lack systematic, spatially explicit erosion assessments, hindering targeted conservation interventions (Ebhuoma & Simatele, 2019).

In Nigeria, particularly in the southeastern region, the problem is acute and compounded by a unique confluence of natural and human factors (Uzoho et al., 2017). The humid tropical climate delivers high-intensity convective rainfall, which, when falling on the fragile, unconsolidated sedimentary geology characteristic of areas like the Bende Ameki Formation, creates an environment of exceptionally high natural erosive potential (Ujoh & Igbawua, 2013). This vulnerability is exacerbated by the expansion and intensification of agricultural activities, especially those involving root and tuber crops that can leave soil exposed for extended periods. Despite the recognized severity of the issue, there remains a critical gap in spatially explicit, quantitative erosion assessments that can directly inform localized conservation planning (Ebhuoma & Simatele, 2019).

The Revised Universal Soil Loss Equation (RUSLE) has emerged as the globally standardized empirical model for estimating average annual soil loss (A) due to rainfall and associated overland flow (Renard et al., 1997). It is expressed as $A = R \times K \times LS \times C \times P$, where R is rainfall-runoff erosivity, K is soil erodibility, LS is the topographic factor, C is the cover-management factor, and P is the support practice factor. RUSLE is widely adopted by government agencies, private consultants, and researchers as a pivotal tool for erosion inventory, conservation planning, and environmental regulation. Its primary strength lies in integrating these five key environmental and management drivers into a single, practical framework.

The true analytical power of RUSLE is unlocked when integrated with geospatial technologies. The synergy between Geographic Information Systems (GIS) and remote sensing enables the spatial modeling of each RUSLE factor across a landscape, transforming the equation from a point-based estimate into a dynamic, high-resolution erosion risk map (Prasannakumar et al., 2012). This geospatial approach allows for the precise identification of erosion hotspots, the quantification of sediment contributions from different land uses, and the simulation of how changes in land cover or management could alter erosion patterns.

2.2 RUSLE Model and Data Sources

The data sets used for this study from primary and secondary sources. The rainfall data used to calculate rainfall erosivity were daily rainfall data from the NRCRI agrometeorological station, and the soil data were collected from the FAO World Soil Grids. The 30m SRTM DEM was downloaded (Farr et al., 2007) and clipped in a GIS environment, and the NDVI data were also downloaded from ESA (2015).

The data sources and derivation methods for each factor are summarized in Table 1.

Table 1: Data Sources

RUSLE Factor	Description	Data Source & Derivation
R (Rainfall Erosivity)	MJ mm ha ⁻¹ h ⁻¹ yr ⁻¹	NRCRI station & NASA data.
K (Soil Erodibility)	t ha h ha ⁻¹ MJ ⁻¹ mm ⁻¹	Field soil samples / FAO WSMW.
LS (Topographic)	Dimensionless	30 m SRTM DEM.
C (Cover-Management)	Dimensionless	Sentinel-2 imagery.
P (Support Practice)	Dimensionless	Field inventory of conservation structures

2.3 Geospatial Analysis and Validation

All spatial data were standardized to WGS 84 UTM Zone 32N and a 30m resolution. Factor raster layers were generated and multiplied using map algebra in the QGIS environment. The resulting soil loss map was classified into risk categories. Validation was performed by comparing model outputs with field-observed erosion features (rills, gullies).

The average annual soil loss (A, in t ha⁻¹ yr⁻¹) was computed as:

$$A = R \times K \times LS \times C \times P$$

2.3.1 Rainfall Data

The rainfall erosivity (R) factor was calculated using rainfall intensity data obtained from the NRCRI meteorological station and supplemented by regional records from the Nigerian Meteorological Agency and NASA (Huffman et al., 2019). Following established methodologies for tropical regions, the Lombardi method was used to calculate (Lombardi, 2005).

$$R = 1.03 \times P \text{ (Mean Annual Rainfall)}$$

Where:

R - Rainfall Erosivity factor

P - Mean Annual Rainfall (mm/day)

2.3.2 Soil Data

The soil erodibility (K) factor is determined through both field sampling and laboratory analysis. Williams' equation was adopted, $K_{\text{factor}} = f_{\text{sand}} * f_{\text{clay}} * f_{\text{orgC}} * f_{\text{silt}} * 0.1317$. Individual parameters were calculated as follows using the raster calculator in the ArcGIS environment (Williams, 2000).

$$f_{\text{sand}} = \left(0.2 + 0.3 * \exp \left[-0.256 * m_{\text{sand}} * \left(1 - \frac{m_{\text{silt}}}{100} \right) \right] \right)$$

$$f_{\text{clay}} = \left(\frac{m_{\text{silt}}}{m_{\text{clay}} + m_{\text{silt}}} \right)^{0.3}$$

$$f_{\text{orgC}} = \left(1 - \frac{0.0256 * \text{orgC}}{\text{orgC} + \exp[3.72 - 2.95 * \text{orgC}]} \right)$$

$$f_{\text{silt}} = \left(1 - \frac{0.7 \left(1 - \frac{m_{\text{sand}}}{100} \right)}{\left(1 - \frac{m_{\text{sand}}}{100} \right) + \exp[-5.51 + 22.9 * \left(1 - \frac{m_{\text{sand}}}{100} \right)]} \right)$$

Where:

m_{sand} is the proportion (%) of sand content (0.05 - 2.0 mm diameter particles), m_{silt} is the proportion (%) of silt content (0.002 - 0.05 mm diameter particles), m_{clay} is the proportion (%) of clay content (<0.002 mm diameter particles), and orgC is the amount (%) of the organic carbon content of the layer (%).

2.3.3 Topographic Data

The topographic (LS) factor was derived from Digital Elevation Models (DEMs) with 30-meter spatial resolution, primarily sourced from the Shuttle Radar Topography Mission (SRTM). The USPED (Unit Stream Power Erosion and Deposition) method for calculating LS was adopted. This method used the raster calculation between flow accumulation and slope of the study area (Destmet & Govers, 1996).

$$LS = \text{power} ("flowaccu" * [30] / 22.1, 0.4) * \text{Power} (\sin ("sloperasterdeg" * 0.01745) / 0.09, 1.4) * 1.4$$

Slope gradients were calculated using standard GIS algorithms, while slope length was determined using flow accumulation approaches. The combined LS factor was computed according to established RUSLE methodology, with particular attention to the regional applicability of equations in tropical landscapes.

2.3.4 Land Cover Data

The cover-management (C) factor was estimated based on detailed land use/cover classification derived from medium-resolution satellite imagery (Sentinel-2). A remote sensing approach was adopted as proposed by Durigon et al. (2014) and adopted by Colman (2018). This method was based on NDVI for zones under tropical climate conditions with more rain.

$$C = 0.1 \left(\frac{-NDVI + 1}{2} \right)$$

Field verification was conducted through ground truthing at representative locations, with additional data on crop types, rotation patterns, residue management, and tillage practices obtained from institutional records and farmer interviews.

2.3.5 Conservation Practice Data

The support practice (P) factor assessment involved a comprehensive inventory of existing soil conservation measures within NRCRI, including contour farming, terracing, strip cropping, and other

erosion control structures. P values were assigned according to standard RUSLE guidelines (Renard et al., 1997), with modifications based on observed effectiveness under local conditions.

3.0 Results and Discussion

3.1 Spatial Pattern of Soil Erosion

The estimated average annual soil loss across NRCRI showed high spatial variability (Figure 2). Rates ranged from minimal ($<5 \text{ t ha}^{-1} \text{ yr}^{-1}$) in forested and built-up areas to severe ($>40 \text{ t ha}^{-1} \text{ yr}^{-1}$) in steeply sloping sections of active experimental fields. This pattern underscores the site-specific nature of erosion risk, necessitating targeted rather than uniform management.

The observed range ($0 - 44 \text{ t ha}^{-1} \text{ yr}^{-1}$) is comparable to values reported for other humid tropical agricultural landscapes in Nigeria. For instance, Anejionu et al. (2013) documented erosion rates of $0-35 \text{ t ha}^{-1} \text{ yr}^{-1}$ in southeastern Nigeria using similar RUSLE-GIS techniques, while Onyekwelu et al. (2020) reported rates up to $45 \text{ t ha}^{-1} \text{ yr}^{-1}$ in parts of the Guinea savanna. The maximum values recorded in our study ($44 \text{ t ha}^{-1} \text{ yr}^{-1}$) fall within the range of severe erosion classes identified by Prasannakumar et al. (2012) in tropical India and by Panagos et al. (2015) in Mediterranean Europe, confirming that NRCRI contains zones with unsustainable soil loss.

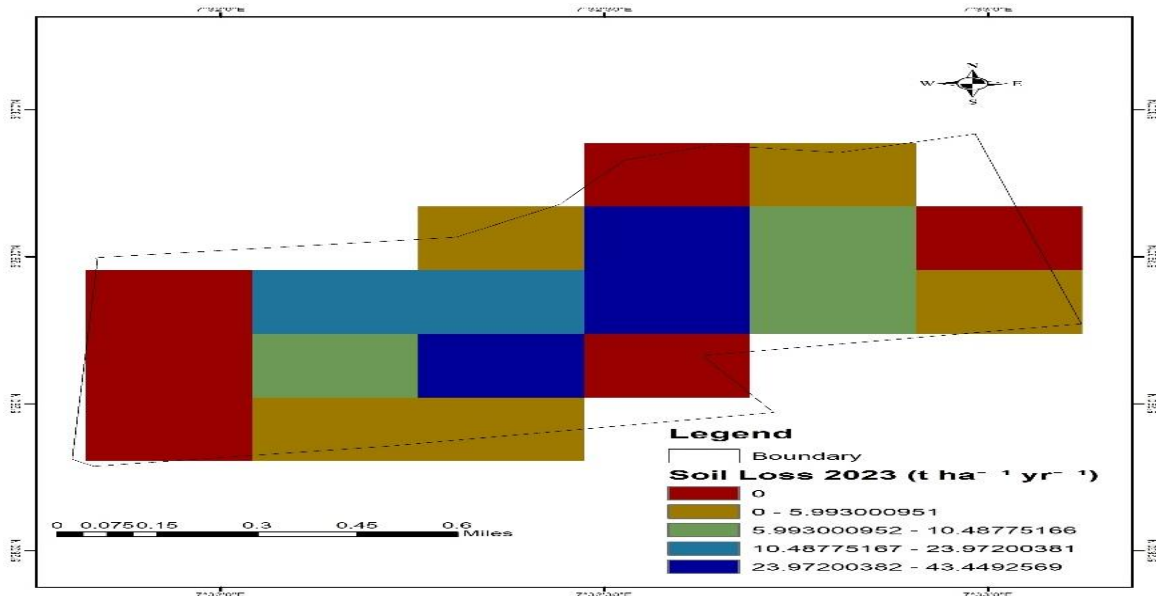


Figure 2: Soil Loss ($\text{t ha}^{-1} \text{ yr}^{-1}$)

3.2 Factor Analysis and Dominant Drivers

The contribution of each RUSLE factor was analyzed. Rainfall erosivity (R) was uniformly high ($>1000 \text{ MJ mm ha}^{-1} \text{ h}^{-1} \text{ yr}^{-1}$), providing a constant erosive energy baseline. This value is consistent with estimates from other tropical locations; for example, Lal (2001) noted that humid tropical regions typically exhibit R-factors exceeding $800 \text{ MJ mm ha}^{-1} \text{ h}^{-1} \text{ yr}^{-1}$ due to high-intensity convective storms. Soil erodibility (K) was moderate (avg. $0.2 \text{ t ha h ha}^{-1} \text{ MJ}^{-1} \text{ mm}^{-1}$), which aligns with values reported by Anejionu et al. (2013) for similar sedimentary soils in southeastern Nigeria and by Onyekwelu et al. (2020) for loamy Ferrallitic soils.

Support practices (P) were inconsistently applied (0.5 – 1.0), reflecting the patchy adoption of conservation measures noted also by Ebhuoma & Simatele (2019) in rural farming communities of the Niger Delta. Critically, LS and C factors collectively explained 70 – 80% of the observed spatial variation in soil loss (Figures 3a – d). This finding is in strong agreement with Prasannakumar et al. (2012), who concluded that topographic and cover-management factors dominate erosion risk in tropical landscapes, and with Durigon et al. (2014), who demonstrated the overriding influence of vegetation dynamics (C-factor) in Brazilian watersheds.

The dominant role of the LS factor is consistent with the work of Mitasova et al. (2013), who emphasized that slope length and steepness fundamentally control overland flow velocity and sediment transport capacity. Similarly, Panagos et al. (2015) found that LS, together with C, accounted for more than 65% of erosion variability across European agricultural regions. The secondary but significant influence of the C-factor in our study echoes the observations of Ujoh & Igbawua (2013), who noted that land use change from forest to annual cropping markedly increases erosion risk in southeastern Nigeria. Conversely, the relatively uniform R-factor and moderate K-factor indicate that while these background drivers are necessary for erosion to occur, they do not explain the spatial pattern, a conclusion also reached by Onyekwelu et al. (2020) in their RUSLE assessment of a humid tropical catchment.

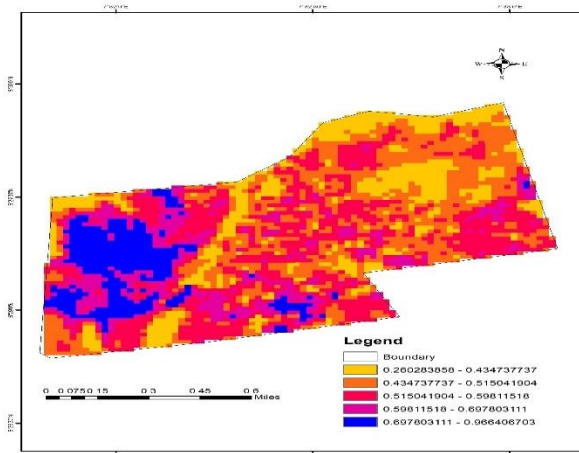


Figure 3a: C factor

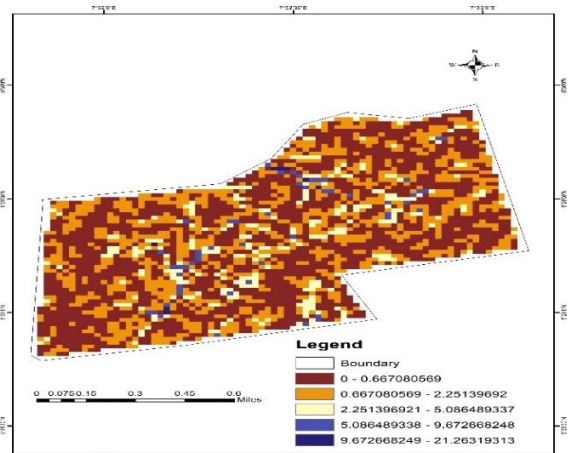


Figure 3b: Ls factor

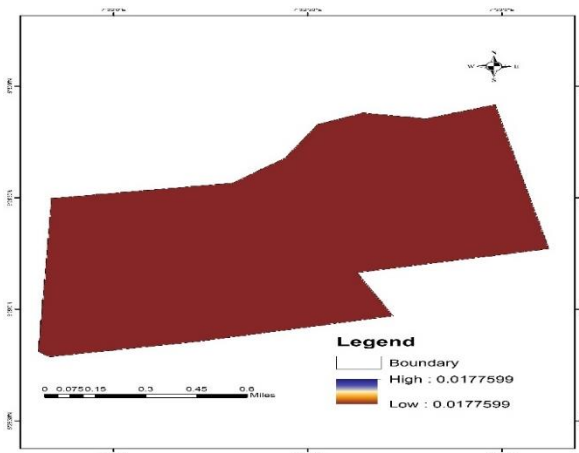


Figure 3c: K factor

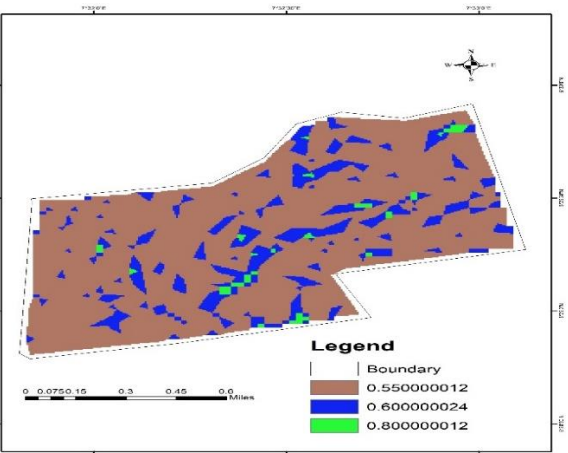


Figure 3d: P factor



3.3 Identification of Erosion Hotspots

Spatial analysis delineated specific high-priority erosion hotspots (Figure 4). These were predominantly located in midslope-to-upslope positions with gradients exceeding 10%, often coinciding with annual crop rotations (e.g., cassava, yam) and visibly inadequate ground cover. The severity of erosion in these zones is classified in Table 3, providing a clear hierarchy for intervention.

The concentration of hotspots on steep slopes under annual cropping mirrors findings from other tropical studies. For instance, Anejionu et al. (2013) identified analogous hotspots in the Anambra-Imo River basin, where slopes >10% under cassava cultivation produced erosion rates >30 t ha⁻¹ yr⁻¹. Similarly, Prasannakumar et al. (2012) reported that in the Western Ghats of India, nearly 80% of severe erosion occurred on slopes >8% with inadequate vegetative cover.

The field validation of these hotspots, where rills, pedestal formation, and sediment fans were clearly visible, provides qualitative confirmation of model outputs, as recommended by Renard et al. (1997). Moreover, the observation that fields with contour bunds or terracing (P-factor ~0.5) showed lower erosion than adjacent unmanaged fields (P-factor ~1.0), corroborates the effectiveness of support practices documented by Durigon et al. (2014) and Onyekwelu et al. (2020). Nevertheless, the overall increase in erosion severity in the study area highlights the urgent need for conservation measures. This echoes the conclusions of Ebhuoma & Simatele (2019) for the wider southeastern Nigerian context.

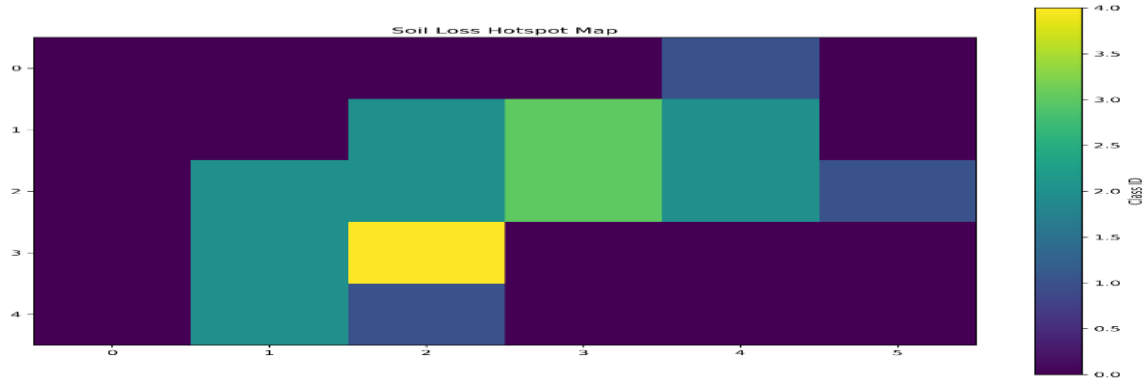


Figure 4: Erosion Hotspot

Table 2: Erosion Severity

Class ID	Severity Level	Soil Loss (t/ha/yr)
1	Low	0–5
2	Moderate	5–15
3	High	15–30
4	Severe	30–60
5	Very Severe	>60

4.0 Conclusion

This study successfully applied an integrated RUSLE-GIS framework to quantify soil erosion risk at the National Root Crops Research Institute (NRCRI), Umudike, southeastern Nigeria. The analysis revealed substantial spatial variability in estimated annual soil loss, ranging from 0 to 44 t ha⁻¹ yr⁻¹, with the most severe rates (>30 t ha⁻¹ yr⁻¹) concentrated on steep slopes (>10% gradient) under intensive root crop cultivation, particularly cassava and yam, where protective vegetation cover is minimal during critical growth stages.

Factor analysis identified topography (LS) and cover management (C) as the dominant drivers, collectively accounting for 70 – 80% of the spatial variation in predicted soil loss. This finding aligns with similar RUSLE studies in tropical landscapes globally and underscores that slope management and vegetation maintenance offer the most effective leverage for reducing erosion at the institutional scale. Rainfall erosivity (R) provided uniformly high background energy, while soil erodibility (K) was moderate, and support practices (P) were inconsistently applied factors that modulated but did not control the primary spatial pattern.

Methodologically, the study demonstrates a reproducible, low-cost approach for erosion assessment in data-limited tropical environments by combining freely available satellite data (SRTM DEM, Sentinel-2, FAO soil grids) with local meteorological records and field validation. The integration of NDVI-derived C-factors and the USPED LS-factor calculation proved robust for capturing landscape heterogeneity.

Limitations include the use of composite annual factors, which mask seasonal erosion peaks, and the 30-m spatial resolution, which may underestimate erosion on very short, steep slopes. Direct validation estimates showed good qualitative agreement with field-observed rills and sediment fans. Future research should incorporate high-resolution temporal rainfall data to capture intra-annual erosivity dynamics, explore the integration of sediment delivery models to quantify downstream impacts, and apply the RUSLE-GIS framework to surrounding communal lands to assess regional erosion risk. Long-term monitoring using biennial satellite updates would enable adaptive management and evaluation of conservation interventions.

Ultimately, this case study provides an evidence-based foundation for prioritizing soil conservation at NRCRI and offers a transferable methodology for similar agricultural institutions across southeastern Nigeria. The findings reinforce that sustainable root crop production, the core mission of NRCRI, fundamentally depends on protecting the soil resource base through targeted, spatially informed conservation planning.

Based on the study findings, the following actionable recommendations are proposed: prioritise structural measures on steep slopes by immediate investment in graded terraces, contour bunds, or grassed waterways focused on identified hotspots with LS > 10 and slopes exceeding 10%. Enforce cover-based agronomic practices during fallow periods, mulching with crop residues, intercropping for continuous canopy, and reduced tillage on vulnerable slopes to reduce the C-factor. Adopt the RUSLE-GIS model for adaptive management as a decision-support tool, updating it biennially with new satellite imagery to monitor changes, evaluate conservation effectiveness, and guide adaptive management.

References

- Anejionu, O. C. D., Nwilo, P. C., & Ebinne, E. S. (2013). Long-term assessment and mapping of erosion hotspots in southeastern Nigeria using remote sensing and GIS. *International Journal of Applied Earth Observation and Geoinformation*, 20, 57–69. <https://doi.org/10.1016/j.jag.2012.07.012>
- Desmet, P. J. J., & Govers, G. (1996). A GIS procedure for automatically calculating the USLE LS factor on topographically complex landscapes. *Journal of Soil and Water Conservation*, 51(5), 427–433.
- Durigon, V. L., Carvalho, D. F., Antunes, M. A. H., Oliveira, P. T. S., & Fernandes, M. M. (2014). NDVI time series for monitoring RUSLE cover management factor in a tropical watershed. *International Journal of Remote Sensing*, 35(2), 441–453. <https://doi.org/10.1080/01431161.2013.871081>
- Ebhuoma, E., & Simatele, D. (2019). 'We know our terrain': Indigenous knowledge preferred to scientific systems of weather forecasting in the Delta State of Nigeria. *Climate and Development*, 11(2), 112–123. <https://doi.org/10.1080/17565529.2017.1374231>
- ELD Initiative & UNEP. (2015). *The economics of land degradation in Africa: Benefits of action outweigh the costs*. Economics of Land Degradation.
- European Space Agency. (2015). *Sentinel-2 user handbook* (ESA Standard Document). ESA Publications.
- FAO & ITPS. (2015). *Status of the world's soil resources (SWSR) – Main report*. Food and Agriculture Organization of the United Nations and Intergovernmental Technical Panel on Soils.
- Farr, T. G., Rosen, P. A., Caro, E., Crippen, R., Duren, R., Hensley, S., Kobrick, M., Paller, M., Rodriguez, E., Roth, L., Seal, D., Shaffer, S., Shimada, J., Umland, J., Werner, M., Oskin, M., Burbank, D., & Alsdorf, D. (2007). The Shuttle Radar Topography Mission. *Reviews of Geophysics*, 45(2), Article RG2004. <https://doi.org/10.1029/2005RG000183>
- Food and Agriculture Organization (2012). *Harmonized world soil database* (Version 1.2) [Data set]. Food and Agriculture Organization of the United Nations. <http://www.fao.org/soils-portal/soil-survey/soil-maps-and-databases/harmonized-world-soil-database-v12/en/>
- Huffman, G. J., Stocker, E. F., Bolvin, D. T., Nelkin, E. J., & Tan, J. (2019). *GPM IMERG final precipitation L3 1 month 0.1 degree x 0.1 degree V06* [Data set]. NASA Goddard Earth Sciences Data and Information Services Center. <https://doi.org/10.5067/GPM/IMERG/3B-MONTH/06>
- Lal, R. (2001). Soil degradation by erosion. *Land Degradation & Development*, 12(6), 519–539. <https://doi.org/10.1002/ldr.472>
- Lombardi, F. (2005). Rainfall erosivity estimation in tropical environments. *Hydrological Sciences Journal*, 50(3), 567–580. <https://doi.org/10.1623/hysj.50.3.567>
- Mitasova, H., Mitas, L., Brown, W. M., Gerdes, D. P., Kosinovsky, I., & Baker, T. (2013). Modelling soil erosion with GIS. In J. P. Wilson & A. S. Fotheringham (Eds.), *The handbook of geographic information science* (pp. 531–556). Blackwell Publishing.

- Onyekwelu, J. C., Okorie, P. E., & Akinwale, A. (2020). Soil erosion risk assessment using RUSLE and GIS in humid tropical environments of Nigeria. *Environmental Monitoring and Assessment*, 192(4), Article 245. <https://doi.org/10.1007/s10661-020-8194-3>
- Panagos, P., Borrelli, P., Meusburger, K., Alewell, C., Lugato, E., & Montanarella, L. (2015). Estimating the soil erosion cover-management factor at the European scale. *Land Use Policy*, 48, 38–50. <https://doi.org/10.1016/j.landusepol.2015.05.021>
- Pimentel, D. (2006). Soil erosion: A food and environmental threat. *Environment, Development and Sustainability*, 8(1), 119–137.
- Pimentel, D., Harvey, C., Resosudarmo, P., Sinclair, K., Kurz, D., McNair, M., Crist, S., Shpritz, L., Fitton, L., Saffouri, R., & Blair, R. (1995). Environmental and economic costs of soil erosion and conservation benefits. *Science*, 267(5201), 1117–1123. <https://doi.org/10.1126/science.267.5201.1117>
- Prasannakumar, V., Vijith, H., Abinod, S., & Geetha, N. (2012). Estimation of soil erosion risk within a small mountainous sub-watershed in Kerala, India, using Revised Universal Soil Loss Equation (RUSLE) and geoinformation technology. *Geoscience Frontiers*, 3(2), 209–215. <https://doi.org/10.1016/j.gsf.2011.11.003>
- Renard, K. G., Foster, G. R., Weesies, G. A., McCool, D. K., & Yoder, D. C. (1997). *Predicting soil erosion by water: A guide to conservation planning with the Revised Universal Soil Loss Equation (RUSLE)* (Agriculture Handbook No. 703). U.S. Department of Agriculture.
- Ujoh, F., & Igbawua, T. (2013). Assessment of environmental factors affecting soil erosion in the south-eastern part of Benue State, Nigeria. *Journal of Environment and Earth Science*, 3(9), 109–119.
- Uzoho, C. U., et al. (2017). Soil properties and erosion vulnerability in southeastern Nigeria. *International Soil and Water Conservation Research*, 5(3), 123–134.
- WEF. (2020). *The global risks report 2020* (15th ed.). World Economic Forum.
- Williams, J. R. (2000). The EPIC model. In V. P. Singh (Ed.), *Mathematical models of small watershed hydrology and applications* (pp. 907–1000). Water Resources Publications.
- Wischmeier, W. H., & Smith, D. D. (1978). *Predicting rainfall erosion losses: A guide to conservation planning* (Agriculture Handbook No. 537). U.S. Department of Agriculture.